



OPEN ACCESS

EDITED BY

Osman Ahmed Zelekew,
Adama Science and Technology
University, Ethiopia

REVIEWED BY

Alemayehu Dubale Duma,
Ethiopian Biotechnology Institute (EBTi),
Ethiopia

Wondimagegne Mengistu,
Bio and Emerging Technology Institute
(BETin), Ethiopia
Rachid Hsissou,
Chouaib Doukkali University, Morocco

*CORRESPONDENCE

Xin Fan,
✉ xfan@glut.edu.cn
Dong Fang,
✉ fangdong@kmust.edu.cn

RECEIVED 26 September 2023

ACCEPTED 13 November 2023

PUBLISHED 13 December 2023

CITATION

Peng D, Fan X and Fang D (2023), High-
efficiency adsorption of Cd²⁺ and Cr³⁺ by
sodium vanadate nanowire arrays.
Front. Mater. 10:1302072.
doi: 10.3389/fmats.2023.1302072

COPYRIGHT

© 2023 Peng, Fan and Fang. This is an
open-access article distributed under the
terms of the [Creative Commons
Attribution License \(CC BY\)](https://creativecommons.org/licenses/by/4.0/). The use,
distribution or reproduction in other
forums is permitted, provided the original
author(s) and the copyright owner(s) are
credited and that the original publication
in this journal is cited, in accordance with
accepted academic practice. No use,
distribution or reproduction is permitted
which does not comply with these terms.

High-efficiency adsorption of Cd²⁺ and Cr³⁺ by sodium vanadate nanowire arrays

Dengzeyu Peng¹, Xin Fan^{1*} and Dong Fang^{2*}

¹College of Materials Science and Engineering, Guilin University of Technology, Guilin, China, ²Faculty of Materials Science and Engineering, Kunming University of Science and Technology, Kunming, China

With the development of economy, the problem of heavy metal pollution in water environment is becoming more and more serious, so it is urgent to find a kind of efficient water purification material. The current work aimed to investigate the potential power of sodium vanadate nanowire arrays (Na₅V₁₂O₃₂) to remove cadmium (Cd²⁺) and chromium (Cr³⁺) from simulated aqueous solutions. The adsorption effects of Na₅V₁₂O₃₂ on Cd²⁺ and Cr³⁺ under different adsorption conditions were analyzed. The products before and after adsorption were compared by XRD, SEM, TEM, FTIR and XPS. The results showed that the irregular grass-like structure of Na₅V₁₂O₃₂ nanowire arrays provided more active sites for the ion exchange reaction, and the maximum adsorption capacity of Cd²⁺ and Cr³⁺ was 541.2 and 251.8 mg·g⁻¹, respectively. The pseudo-second-order kinetic model was more suitable to describe the adsorption behavior by kinetic study. The research demonstrated that Na₅V₁₂O₃₂ nanowire arrays exhibited excellent adsorption performance, which provided an effective parameter basis for the future adsorption of heavy metal ions.

KEYWORDS

Na₅V₁₂O₃₂, nanowire array, adsorption, heavy metal ions, kinetic study

1 Introduction

With the rapid economic developments, the ecological environment we live in is gradually being destroyed, and heavy metal pollution in water from metallurgy, mining, and other industries has aroused wide concern all over the world (Bensalah et al., 2023; Jebli et al., 2023; Lebkiri et al., 2023). Cadmium (Cd²⁺) and chromium (Cr³⁺) are common toxic heavy metals and have been identified as harmful to the human body (Elfeghe et al., 2022; Kocaoba et al., 2022). Studies have shown that small amounts of chromium and cadmium can have a significant toxic effect on humans (El Gaayda et al., 2023). In addition, chromium and cadmium can cause more serious health problems and even death after accumulation because the human body finds them difficult to discharge (Makarenko et al., 2019; Shahryari et al., 2019). Therefore, how to remove these heavy metal ions becomes extremely urgent.

Recently, a variety of effective methods have been developed to remove heavy metal ions from water, such as chemical precipitation (Wu, 2019), electrochemical treatment (Liu et al., 2019a), solvent extraction (Ishfaq et al., 2019), membrane separation (Song et al., 2022), and ion exchange (Rengaraj et al., 2002; Bentouami and Oulai, 2006; Elkady et al., 2011; Arim et al., 2018; Liu et al., 2019b; Priastomo et al., 2020). In the above methods, the ion exchange technique is the most widely used method in removing heavy metal ions because it is environmentally friendly, economically applicable, renewable, and highly efficient. Elkady et al. (Elkady et al., 2011) prepared nano-poly (glycidyl methacrylate) cation exchange resin to remove Cd²⁺ and the



FIGURE 1
Preparation process diagram of $\text{Na}_5\text{V}_{12}\text{O}_{32}$ nanowire arrays.

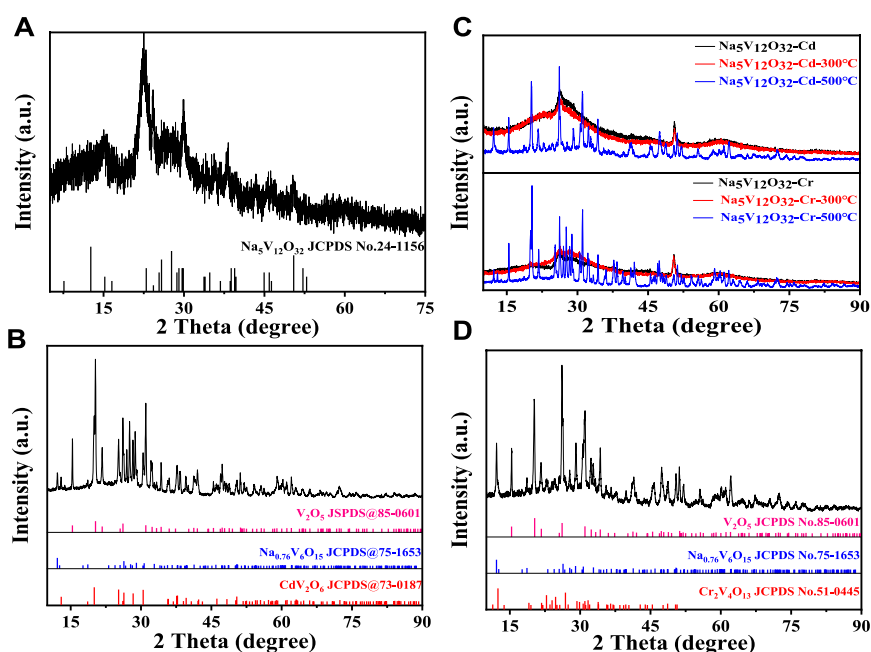


FIGURE 2
XRD patterns of products before and after adsorption: (A) $\text{Na}_5\text{V}_{12}\text{O}_{32}$, (B) $\text{Na}_5\text{V}_{12}\text{O}_{32}\text{-Cd-500}^\circ\text{C}$, (C) $\text{Na}_5\text{V}_{12}\text{O}_{32}\text{-Cd}$ and $\text{Na}_5\text{V}_{12}\text{O}_{32}\text{-Cr}$ at different temperatures, (D) $\text{Na}_5\text{V}_{12}\text{O}_{32}\text{-Cr-500}^\circ\text{C}$.

adsorption capacity could reach 90%. The results showed that initial cadmium concentration, pH value, and resin dosage had a great influence on adsorption. Bentouami et al. (Bentouami and Oulai, 2006) modified the bentonite and prepared bentonite-oxine complex for cadmium removal. After the batch test, the maximum adsorption capacity reached $61.35 \text{ mg}\cdot\text{g}^{-1}$. Liu et al. (Liu et al., 2019b) synthesized an eco-friendly gamma-cyclodextrin metal-organic framework (MOF)-based nanoporous carbon material to remove Cd^{2+} from the solution, and used the Langmuir model to calculate the maximum adsorption capacity which was $140.85 \text{ mg}\cdot\text{g}^{-1}$. Ion exchange technology can also be used to remove chromium ions. Rengaraj et al. (Rengaraj et al., 2002) studied the adsorption of Cr^{3+} by IRN77 cation-exchange resin, and it was found that the adsorption efficiency could exceed 95% under the best reaction conditions. Arim et al. (Arim et al., 2018) found that chemically modified pine bark had a good adsorption effect on chromium. Under the action of ion exchange, the maximum

adsorption capacity was $31.40 \text{ mg}\cdot\text{g}^{-1}$ when pH was 5. Jumina et al. (Priastomo et al., 2020) successfully prepared a simple adsorbent named C-Phenylcalix (Elfeghe et al., 2022) pyrogallolarene, and evaluated for the simultaneous adsorption of Cr^{3+} in acidic media. The results indicated that the adsorption capacity of Cr^{3+} was found to be $14.31 \text{ mg}\cdot\text{g}^{-1}$. However, there are still some problems regarding the aforementioned adsorbent materials, which have complex preparation and relatively low adsorption capacity (Kadiri et al., 2021; El amri et al., 2023). Therefore, adsorbent materials with low cost, high performance, and simple preparation are highly required.

In the present study, sodium vanadate ($\text{Na}_5\text{V}_{12}\text{O}_{32}$) nanowire arrays were fabricated by means of a hydrothermal method. The samples were characterized by using scanning electron microscopy, Fourier transform infrared spectrum, and X-ray diffraction. Different methods were used to characterize the $\text{Na}_5\text{V}_{12}\text{O}_{32}$ nanowire arrays before and after the adsorption of Cd^{2+} and Cr^{3+} . By examining the

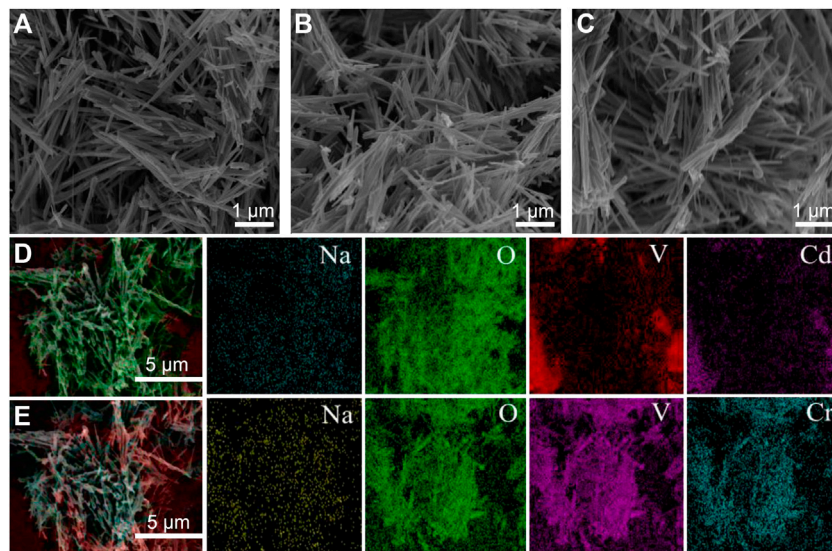


FIGURE 3 SEM images of (A) $\text{Na}_5\text{V}_{12}\text{O}_{32}$, (B) $\text{Na}_5\text{V}_{12}\text{O}_{32}\text{-Cd}$, (C) $\text{Na}_5\text{V}_{12}\text{O}_{32}\text{-Cr}$, (D) and (E) are the element mapping images of $\text{Na}_5\text{V}_{12}\text{O}_{32}\text{-Cd}$ and $\text{Na}_5\text{V}_{12}\text{O}_{32}\text{-Cr}$, respectively.

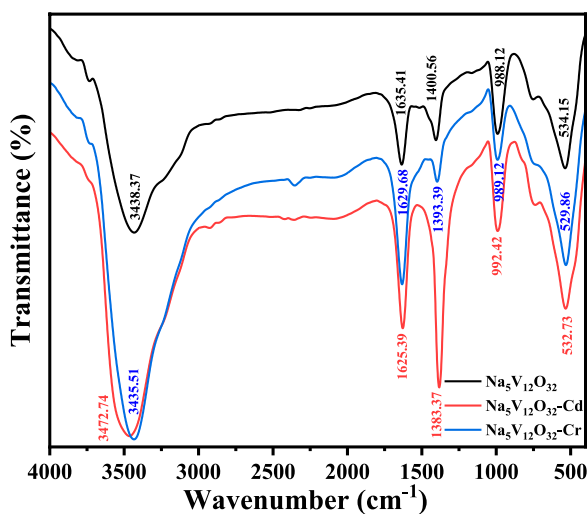


FIGURE 4 FTIR of $\text{Na}_5\text{V}_{12}\text{O}_{32}$ nanowire arrays before and after adsorption.

effects of adsorbent dosage and adsorption time during the adsorption experiments to confirm the advantage of $\text{Na}_5\text{V}_{12}\text{O}_{32}$ nanowire arrays.

2 Materials and methods

2.1 Materials

Ammonium metavanadate (NH_4VO_3 , $\geq 99.9\%$), sodium chloride (NaCl , $\geq 99.9\%$), oxalic acid ($\text{H}_2\text{C}_2\text{O}_4$, $\geq 99.9\%$), hexamethylene tetramine ($\text{C}_6\text{H}_{12}\text{N}_4$, HMTA, $\geq 99.7\%$), cadmium nitrate (CdN_2O_6 , $\geq 99.9\%$), and chromium trichloride (CrCl_3 , $\geq 99.9\%$) were all purchased from the

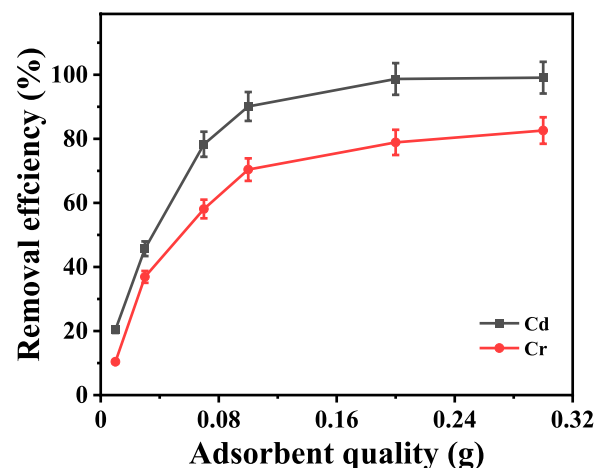
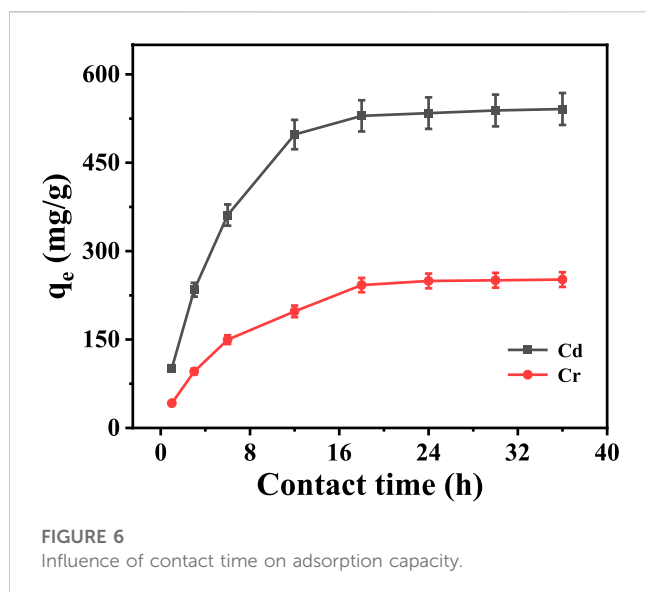


FIGURE 5 Effect of adsorbent dosage on the removal.

Sinopharm. Co. Ltd. All chemicals were used as received. Deionized water was prepared in the laboratory. The simulated wastewater containing Cd^{2+} and Cr^{3+} was prepared by dissolving amounts of CdN_2O_6 and CrCl_3 in deionized water, respectively.

2.2 Preparation of $\text{Na}_5\text{V}_{12}\text{O}_{32}$ nanowire arrays

As shown in Figure 1, $\text{Na}_5\text{V}_{12}\text{O}_{32}$ nanowire arrays were prepared by a hydrothermal method (Cao et al., 2015). Ammonium metavanadate, sodium chloride, oxalic acid, and HMTA in a molar ratio of 1:6:2:0.2 were mixed in proportion



with deionized water and stirred for 6 h to obtain the precursor solution. Then the precursor solution was added into a 25 mL polytetrafluoroethylene stainless steel autoclave (adding Ti foils), and heated 150°C for 1 h to synthesize $\text{Na}_5\text{V}_{12}\text{O}_{32}$ nanowire arrays on Ti foil. After the reaction, the Ti foils were taken out when the temperature cooled down to room temperature, and the samples were washed and dried to obtain $\text{Na}_5\text{V}_{12}\text{O}_{32}$ nanowire arrays.

2.3 Characterization methods

X-ray diffraction (XRD, BrukerD8) was applied to check the possible composition of the samples before and after use. A scanning electron microscope (SEM, Hitachi) with an energy dispersive spectrometer (EDS) was used to analyze surface morphology and

chemical elements composition. The structure of the products was characterized by transmission electron microscopy (TEM, Tecnai G2 F30S-TWIN). The chemical compositions of the samples were analyzed by X-ray photoelectron spectroscopy (XPS, KAlpha 1063). Fourier transform infrared spectroscopy (FTIR, ALPHA) was employed to investigate the functional groups of the sample. The concentration of metal ions in the solution was acquired by inductively coupled plasma optical emission spectroscopy (ICP-OES, 7400).

2.4 Adsorption experiments

Stock solution A containing 1000 $\text{mg}\cdot\text{L}^{-1}$ Cd^{2+} was prepared by dissolving CdN_2O_6 in distilled water. Similarly, stock solution B containing 1000 $\text{mg}\cdot\text{L}^{-1}$ Cr^{3+} was obtained by adding CrCl_3 . Then, the desired solutions were prepared by dilution of the stock solution.

A series of adsorption experiments of $\text{Na}_5\text{V}_{12}\text{O}_{32}$ nanowire arrays on the desired solutions were conducted, and the samples after adsorption were named $\text{Na}_5\text{V}_{12}\text{O}_{32}\text{-Cd}$ and $\text{Na}_5\text{V}_{12}\text{O}_{32}\text{-Cr}$. The adsorption capacity of sodium vanadate was evaluated by the adsorbent dose and adsorption time. All experiments were performed at room temperature. After the reaction, the supernatant was collected for characterization and analysis, and the amount of adsorption was determined by ICP.

2.5 Kinetic study of adsorption

Sodium vanadate was used to adsorb heavy metal ions (Cd^{2+} and Cr^{3+}) to determine the adsorption equilibrium time. At the stirring speed of 150 rpm, 0.1 g of $\text{Na}_5\text{V}_{12}\text{O}_{32}$ was added to a solution of heavy metal ions with a concentration of 4,000 $\text{mg}\cdot\text{L}^{-1}$. The equilibrium adsorption capacity was calculated by the following equation (Eq. 1):

TABLE 1 Comparison of the maximum adsorption capacity for Cd^{2+} and Cr^{3+} .

Adsorbent	Ion type	Q_{max} ($\text{mg}\cdot\text{g}^{-1}$)	Source
$\text{Na}_5\text{V}_{12}\text{O}_{32}$	Cd^{2+}	541.2	This work
Bentonite	Cd^{2+}	61.4	Bentouami and Oulai (2006)
Nanoporous carbon	Cd^{2+}	140.9	Liu et al. (2019b)
Magnetic hydrogel	Cd^{2+}	308.8	Zhu et al. (2016)
PAM hydrogel	Cd^{2+}	216.2	Lebkiri et al. (2022)
Waste bovine bone	Cd^{2+}	79.0	Wang et al. (2023)
$\text{Na}_5\text{V}_{12}\text{O}_{32}$	Cr^{3+}	251.8	This work
Modified pine bark	Cr^{3+}	31.4	Arim et al. (2018)
Active carbon	Cr^{3+}	14.3	Priastomo et al. (2020)
Polyamide nanofibers	Cr^{3+}	79.5	Zhang et al. (2020)
Modified sodium alginate	Cr^{3+}	157.6	Wen et al. (2022)
rGO- Mn_3O_4	Cr^{3+}	138.5	Lingamdinne et al. (2022)

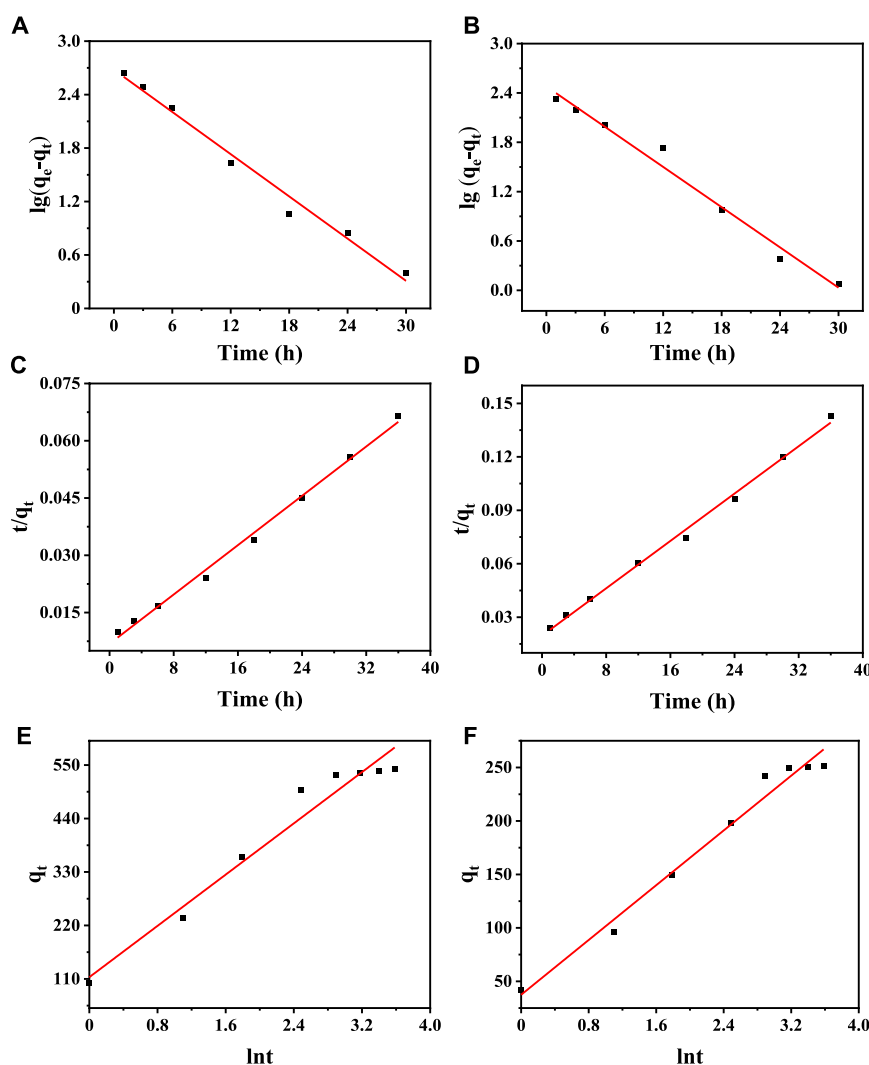


FIGURE 7

Kinetic simulation of $\text{Na}_5\text{V}_{12}\text{O}_{32}$ adsorption: Pseudo first order kinetic diagram of Cd^{2+} (A) and (B) Cr^{3+} adsorbed on $\text{Na}_5\text{V}_{12}\text{O}_{32}$; Pseudo second order kinetic diagram of (C) Cd^{2+} and (D) Cr^{3+} adsorbed on $\text{Na}_5\text{V}_{12}\text{O}_{32}$; Elovich kinetics diagram of (E) Cd^{2+} and (F) Cr^{3+} adsorbed on $\text{Na}_5\text{V}_{12}\text{O}_{32}$.

$$q_e = \frac{(C_0 - C) \times V}{W} \quad (1)$$

where, q_e ($\text{mg}\cdot\text{g}^{-1}$) is the amount of heavy metals adsorbed in equilibrium, w (g) is the amount of adsorbent, c_0 and c ($\text{mg}\cdot\text{L}^{-1}$) are the initial and equilibrium concentrations of heavy metal ions, and v (L) is the volume of the heavy metal ion solution.

3 Results and discussion

3.1 Characterization of the adsorbent

The $\text{Na}_5\text{V}_{12}\text{O}_{32}$ nanowire arrays of 0.1 g which reacted with the desired solution (the concentration of Cd^{2+} or Cr^{3+} was $4,000 \text{ mg}\cdot\text{L}^{-1}$) under stirring at 25°C were tested. The X-ray diffraction spectrum of the products before and after adsorption is shown in Figure 2. In Figure 2A, the prepared $\text{Na}_5\text{V}_{12}\text{O}_{32}$ nanowire arrays had low crystallinity at room temperature, and the peaks near 15.2° , 22.8° , 29.8° , 38.8° , and 50.3°

correspond to (200), (300), (-211) , (-303) , and (020) crystal faces of $\text{Na}_5\text{V}_{12}\text{O}_{32}$ (JCPDS No.24-1156), respectively. In order to analyze the structure and composition of the adsorbed products more accurately, the adsorbed products were heated at different temperatures, and named $\text{Na}_5\text{V}_{12}\text{O}_{32}\text{-Cd-}300^\circ\text{C}$, $\text{Na}_5\text{V}_{12}\text{O}_{32}\text{-Cd-}500^\circ\text{C}$, $\text{Na}_5\text{V}_{12}\text{O}_{32}\text{-Cr-}300^\circ\text{C}$, and $\text{Na}_5\text{V}_{12}\text{O}_{32}\text{-Cr-}500^\circ\text{C}$, respectively, and are shown in Figure 2B. With the increase in temperature, the crystallinity of $\text{Na}_5\text{V}_{12}\text{O}_{32}\text{-Cd}$ and $\text{Na}_5\text{V}_{12}\text{O}_{32}\text{-Cr}$ improved, the diffraction peak became more acute, and the signals of many other peaks were displayed. In Figure 2C, the peaks of the sample belong to CdV_2O_6 (JCPDS No.73-0187), V_2O_5 (JCPDS No.73-0187), and $\text{Na}_{0.76}\text{V}_6\text{O}_{15}$ (JCPDS No.75-1653) which showed that an ion exchange reaction occurred between Cd^{2+} and $\text{Na}_5\text{V}_{12}\text{O}_{32}$ to produce CdV_2O_6 . Furthermore, the incompleteness of the chemical reaction was confirmed by the appearance of V_2O_5 and $\text{Na}_{0.76}\text{V}_6\text{O}_{15}$. Similar results can be seen in Figure 2D as CrCl_3 was converted to $\text{Cr}_2\text{V}_4\text{O}_{13}$ due to ion exchange. The peaks of the sample belong to V_2O_5 (JCPDS No.73-0187) and $\text{Na}_{0.76}\text{V}_6\text{O}_{15}$ (JCPDS No.75-1653), which could also be ascribed to an incomplete ion exchange.

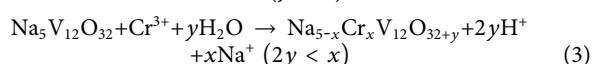
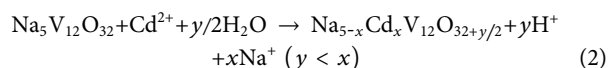
TABLE 2 Kinetic parameters of the adsorption of Na₅V₁₂O₃₂ to Cd²⁺ and Cr³⁺.

	Pseudo-first-order dynamic		Pseudo-second-order dynamic		Elovich dynamic		
	<i>k</i> ₁	<i>R</i> ²	<i>k</i> ₂	<i>R</i> ²	<i>α</i>	<i>β</i>	<i>R</i> ²
Cd ²⁺	0.18781	0.9833	5.789 × 10 ⁻⁴	0.9945	311.991	7.583 × 10 ⁻³	0.9541
Cr ³⁺	0.18191	0.9792	3.795 × 10 ⁻⁴	0.9949	114.878	1.561 × 10 ⁻³	0.9776

The surface morphology of the samples was further studied using an SEM and the results are shown in Figure 3. As can be seen from Figure 3A, the surface of Na₅V₁₂O₃₂ nanowire arrays was relatively smooth and showed an irregular grass-like structure which could increase the number of active sites, and the assays achieved efficient adsorption of Cd²⁺ and Cr³⁺ through ion exchange reaction. Supplementary Figure S1 shows the prepared Na₅V₁₂O₃₂ nanowire arrays on a nanometer scale and the diameter was 157 nm.

The SEM images of the adsorbed product are shown in Figures 3B, C. The results showed that the structure of the Na₅V₁₂O₃₂ nanowire arrays was stable, and there was no obvious change before and after adsorption. The volume of sodium vanadate after adsorption was slightly larger, and a small number of particles were attached to the surface. The element mapping images of Na₅V₁₂O₃₂-Cd and Na₅V₁₂O₃₂-Cr are shown in Figures 3D, E. The appearance of Cd and Cr proved the successful adsorption of Na₅V₁₂O₃₂, and the sodium element indicated that the ion exchange reaction was incomplete, which was consistent with the results shown in Supplementary Figure S2.

In order to further verify the adsorption mechanism, the FTIR of Na₅V₁₂O₃₂, Na₅V₁₂O₃₂-Cd, and Na₅V₁₂O₃₂-Cr were investigated and compared, and are shown in Figure 4. The characteristic adsorption peaks of the Na₅V₁₂O₃₂ nanowire arrays (Vatanpour et al., 2021) were located at 1635.41 cm⁻¹ and 1400.56 cm⁻¹ (V-OH symmetrical tensile vibration and anti-symmetrical tensile vibration), 988.12 cm⁻¹ (V=O tensile vibration), and 534.15 cm⁻¹ (V-O-V symmetrical tensile vibration). After Cr³⁺ adsorption, the peaks mainly existed at 1629.68, 1393.39, 989.12, and 529.86 cm⁻¹, and after Cd²⁺ adsorption, the peaks mainly existed at 1625.39, 1383.37, 992.42, and 532.73 cm⁻¹. This indicated that before and after adsorption, the peaks had a small shift, which could be attributed to the stability of the vanadate structure and no change of functional group in the reaction. The characteristic sorption peaks at 1635.41 cm⁻¹ were strong after the adsorption. This could be explained by the fact that V-OH vibration was strengthened after the ion exchange of Na⁺ to Cd²⁺ and Cr³⁺, making the corresponding bands strong (Harbi et al., 2016). The change in the peak at 1383.37 cm⁻¹ was more obvious than that at 1393.39 cm⁻¹, which could be due to the higher adsorption capacity. During the ion exchange process (Fang et al., 2021), the reaction equation (Eqs 2, 3) could be described as follows:



3.2 Adsorption test

3.2.1 Effect of adsorbent dose

In order to explore the effect of adsorbent on the experiment, a series of adsorption experiments were conducted with different adsorbents with mass and an initial concentration of 100 mg·L⁻¹. Figure 5 shows the effect of adsorbent dosage on the removal of Cd²⁺ and Cr³⁺. The results showed that with the increase in the dosage of Na₅V₁₂O₃₂, the removal rate of Cd²⁺ and Cr³⁺ also increased, but the adsorption rate gradually slowed down. When the amount of adsorbent was 0.1 g, the removal rate of Cd²⁺ was increased by 90.1%, and when the amount of adsorbent was increased to 0.3 g, the removal rate of Cd²⁺ was 99.1%, which was only an increase of 9 percentage points. The same situation could also be found in the removal of Cr³⁺, as when the amount of adsorbent was 0.1 g, the removal rate of Cr³⁺ was increased by 70.4%, and when the amount of adsorbent increased to 0.3 g, the removal rate was 82.6%, which was only an increase of 12.6 percentage points. Therefore, 0.1 g was the best amount of adsorbent.

3.2.2 Effect of adsorption time

In order to explore the effect of adsorption time on the experiment, a series of adsorption experiments were conducted with different contact times and an initial concentration of 4,000 mg·L⁻¹.

Figure 6 shows the influence of contact time on adsorption capacity. It indicates that the adsorption capacity of Na₅V₁₂O₃₂ on Cd²⁺ and Cr³⁺ increased rapidly with the increase of contact time, and then tended to be stable. When the contact time was 36 h, the maximum adsorption capacity was 541.2 and 251.8 mg·g⁻¹, respectively. This can be attributed to the gradual reduction of the ion exchange site of Na₅V₁₂O₃₂ with the progress of the reaction, which makes the adsorption rate gradually decrease and finally tends to the adsorption equilibrium.

At the same time, the adsorption capacity of sodium vanadate was compared and is shown in Table 1. Compared with other adsorbents, the Na₅V₁₂O₃₂ nanowire arrays in this study had a higher maximum adsorption capacity and were adsorbent with excellent adsorption performance to remove heavy metal ions from aqueous solution.

3.3 Adsorption kinetics

The analysis of adsorption kinetics was used to determine the adsorption rate and the equilibrium time during ion exchange. The adsorption of Cd²⁺ and Cr³⁺ by Na₅V₁₂O₃₂ is a complex process, and the main behavior and mechanism of the adsorption process can be analyzed by certain models. In this experiment, a pseudo-first-order dynamic model (Dao et al., 2022), pseudo-second-order dynamic model (Khamizov, 2020), and Elovich dynamic model (Kaki et al., 2019) were established to find the most suitable model for the

experimental data, and the results are shown in Figure 7. The kinetic parameters and correlation coefficients are shown in Table 2. The results show that the R^2 values of the pseudo-second-order kinetic model are 0.9945 and 0.9949, respectively, which are much higher than those of the pseudo-first-order kinetic model and Elovich kinetic model. Therefore, the pseudo-second-order kinetic model is more suitable to describe the adsorption behavior of Cd^{2+} and Cr^{3+} by $\text{Na}_5\text{V}_{12}\text{O}_{32}$.

4 Conclusion

In this experiment, sodium vanadate nanowire arrays ($\text{Na}_5\text{V}_{12}\text{O}_{32}$) were synthesized by a simple hydrothermal method and used as an adsorbent to remove Cd^{2+} and Cr^{3+} from the simulated solution. The adsorption experiment results showed that the $\text{Na}_5\text{V}_{12}\text{O}_{32}$ nanowire arrays had great adsorption potential, and the maximum adsorption capacity of Cd^{2+} and Cr^{3+} was 541.2 and 251.8 $\text{mg}\cdot\text{g}^{-1}$, respectively. The adsorption behavior was more consistent with the pseudo-second-order kinetic model. In summary, $\text{Na}_5\text{V}_{12}\text{O}_{32}$ nanowire arrays are a promising candidate for heavy metal ion wastewater treatment, and the high adsorption performance is worthy of further exploration and research.

Data availability statement

The original contributions presented in the study are included in the article/Supplementary Material, further inquiries can be directed to the corresponding authors.

Author contributions

DP: Writing—original draft. XF: Supervision, Visualization, Writing—review and editing. DF: Supervision, Writing—review and editing.

References

- Arim, A. L., Quina, M. J., and Gando-Ferreira, L. M. (2018). Insights into the sorption mechanisms of Cr(III) by chemically modified pine bark. *Chem. Eng. Technol.* 41 (7), 1378–1389. doi:10.1002/ceat.201800034
- Bensalah, J., Idrissi, A., Faydy, M. E., Doumane, G., Staoui, A., Hsissou, R., et al. (2023). Investigation of the cationic resin as a potential adsorbent to remove MR and CV dyes: kinetic, equilibrium isotherms studies and DFT calculations. *J. Mol. Struct.* 1278, 134849. doi:10.1016/j.molstruc.2022.134849
- Bentouami, A., and Oulai, M. S. (2006). Cadmium removal from aqueous solutions by hydroxy-8 quinoline intercalated bentonite. *J. Colloid Interface Sci.* 293 (2), 270–277. doi:10.1016/j.jcis.2005.06.040
- Cao, Y., Fang, D., Wang, C., Xu, W., Luo, Z., et al. (2015). Novel aligned sodium vanadate nanowire arrays for high-performance lithium-ion battery electrodes. *Rsc Adv.* 5 (53), 42955–42960. doi:10.1039/c5ra01102g
- Dao, P. T., Tran, N. Y. T., Tran, Q. N., Bach, G. L., and Lam, T. V. (2022). Kinetics of pilot-scale essential oil extraction from pomelo (*Citrus maxima*) peels: Comparison between linear and nonlinear models. *Alexandria Eng. J.* 61 (3), 2564–2572. doi:10.1016/j.aej.2021.07.002
- el Amri, A., Kadiri, L., Hsissou, R., Lebki, A., Wardighi, Z., Rifi, E. H., et al. (2023). Investigation of Typha Latifolia (TL) as potential biosorbent for removal of the methyl orange anionic dye in the aqueous solution. Kinetic and DFT approaches. *J. Mol. Struct.* 1272, 134098. doi:10.1016/j.molstruc.2022.134098
- Elfegh, S., Anwar, S., and Zhang, Y. H. (2022). Adsorption and removal studies of cadmium ion onto sulphonic/phosphonic acid functionalization resins. *Can. J. Chem. Eng.* 100 (10), 3006–3014. doi:10.1002/cjce.24400
- el Gaayda, J., Rachid, Y., Titchou, F. E., Barra, I., Hsini, A., Yap, P. S., et al. (2023). Optimizing removal of chromium (VI) ions from water by coagulation process using central composite design: effectiveness of grape seed as a green coagulant. *Sep. Purif. Technol.* 307, 122805. doi:10.1016/j.seppur.2022.122805
- Elkady, M. F., Abu-Saied, M. A., Rahman, A. M. A., Soliman, E., Elzatahry, A., Elsayed Youssef, M., et al. (2011). Nano-sulphonated poly (glycidyl methacrylate) cations exchanger for cadmium ions removal: effects of operating parameters. *Desalination* 279 (1–3), 152–162. doi:10.1016/j.desal.2011.06.002
- Fang, D., Xu, X., Bao, R., Wan, R., Yang, F., Yi, J., et al. (2021). Layered $\text{Na}_5\text{V}_{12}\text{O}_{32}$ nanowires with enhanced properties of removing Pb^{2+} in aqueous solution by chemical reaction. *J. Environ. Chem. Eng.* 9 (2), 104765. doi:10.1016/j.jece.2020.104765
- Harbi, S., Guesmi, F., Tabassi, D., Hannachi, C., and Hamrouni, B. (2016). Application of response surface methodology and artificial neural network: modeling and optimization of Cr(VI) adsorption process using Dowex 1X8 anion exchange resin. *Water Sci. Technol.* 73 (10), 2402–2412. doi:10.2166/wst.2016.091
- Ishfaq, A., Ilyas, S., Yaseen, A., and Farhan, M. (2019). Hydrometallurgical valorization of chromium, iron, and zinc from an electroplating effluent. *Sep. Purif. Technol.* 209, 964–971. doi:10.1016/j.seppur.2018.09.050
- Jebli, A., Amri, A. E., Hsissou, R., Lebki, A., Zarrik, B., Bouhassane, F. Z., et al. (2023). Synthesis of a chitosan@hydroxyapatite composite hybrid using a new approach for high-performance removal of crystal violet dye in aqueous solution, equilibrium isotherms and process optimization. *J. Taiwan Inst. Chem. Eng.* 149, 105006. doi:10.1016/j.jtice.2023.105006

Funding

The author(s) declare financial support was received for the research, authorship, and/or publication of this article. This work was supported by the fund of the Key Special Projects of the Ministry of Science and Technology (China: 2021YFE0104300, Uzbekistan: MUK-2021-45), Major Special Projects in Yunnan Province (No. 202002AB080001), Science Research Project of Yunnan Province (No. 202001AT070082), Basic Research Project of Yunnan Province/General Project (No. 202001AT070002), and Kunming Academician Expert Workstation of Yunnan Province.

Conflict of interest

The authors declare that the research was conducted in the absence of any commercial or financial relationships that could be construed as a potential conflict of interest.

Publisher's note

All claims expressed in this article are solely those of the authors and do not necessarily represent those of their affiliated organizations, or those of the publisher, the editors and the reviewers. Any product that may be evaluated in this article, or claim that may be made by its manufacturer, is not guaranteed or endorsed by the publisher.

Supplementary material

The Supplementary Material for this article can be found online at: <https://www.frontiersin.org/articles/10.3389/fmats.2023.1302072/full#supplementary-material>

- Kadiri, L., Ouass, A., Hsissou, R., Safi, Z., Wazzan, N., Essaadaoui, Y., et al. (2021). Adsorption properties of coriander seeds: spectroscopic kinetic thermodynamic and computational approaches. *J. Mol. Liq.* 343, 116971. doi:10.1016/j.molliq.2021.116971
- Kaki, E., Gogsu, N., Altindal, A., Salih, B., and Bekaroğlu, Ö. (2019). Synthesis, characterization and VOCs adsorption kinetics of diethylstilbestrol-substituted metallophthalocyanines. *J. Porphy. Phthalocyanines* 23 (1-2), 166–174. doi:10.1142/s1088424619500196
- Khamizov, R. K. A. (2020). A pseudo-second order kinetic equation for sorption processes. *Russ. J. Phys. Chem. A* 94 (1), 171–176. doi:10.1134/s0036024420010148
- Kocaoba, S., Cetin, G., and Akcin, G. (2022). Chromium removal from tannery wastewaters with a strong cation exchange resin and species analysis of chromium by MINEQL+. *Sci. Rep.* 12 (1), 9618. doi:10.1038/s41598-022-14423-3
- Lebkiri, I., Abbou, B., Hsissou, R., Safi, Z., Sadiku, M., Berisha, A., et al. (2023). Investigation of the anionic polyacrylamide as a potential adsorbent of crystal violet dye from aqueous solution: equilibrium, kinetic, thermodynamic, DFT, MC and MD approaches. *J. Mol. Liq.* 372, 121220. doi:10.1016/j.molliq.2023.121220
- Lebkiri, I., Abbou, B., Kadiri, L., Ouass, A., Essaadaoui, Y., Ouaddari, H., et al. (2022). Polyacrylamide hydrogel an effective adsorbent for the removal of heavy metal from aqueous solution: isotherm, kinetic, and thermodynamic studies. *Russ. J. Phys. Chem. A* 96 (7), 1484–1492. doi:10.1134/s0036024422070159
- Lingamdinne, L. P., Godlaveeti, S. K., Angaru, G. K. R., Chang, Y. Y., Nagireddy, R. R., Somala, A. R., et al. (2022). Highly efficient surface sequestration of Pb²⁺ and Cr³⁺ from water using a Mn₃O₄ anchored reduced graphene oxide: selective removal of Pb²⁺ from real water. *Chemosphere* 299, 134457. doi:10.1016/j.chemosphere.2022.134457
- Liu, C., Wang, P., Liu, X. K., Yi, X., Liu, D., and Zhou, Z. (2019b). Ultrafast removal of Cadmium(II) by green cyclodextrin metal-organic-framework-based nanoporous carbon: adsorption mechanism and application. *Chemistry-an Asian J.* 14 (2), 261–268. doi:10.1002/asia.201801431
- Liu, C., Wu, T., Hsu, P. C., Xie, J., Zhao, J., Liu, K., et al. (2019a). Direct/alternating current electrochemical method for removing and recovering heavy metal from water using graphene oxide electrode. *ACS Nano* 13 (6), 6431–6437. doi:10.1021/acsnano.8b09301
- Makarenko, N. V., Arefieva, O. D., Kovekhova, A. V., and Zemnukhova, L. A. (2019). Removal of Cr³⁺ ions by phytic acid derivatives from rice bran. *Bioresources* 14 (2), 4866–4872. doi:10.15376/biores.14.2.4866-4872
- Priastomo, Y., Setiawan, H. R., Mutmainah, Kurniawan, Y. S., and Ohto, K. (2020). Simultaneous removal of lead(II), chromium(III), and copper(II) heavy metal ions through an adsorption process using C-phenylcalix 4 pyrogallolarene material. *J. Environ. Chem. Eng.* 8 (4), 103971. doi:10.1016/j.jece.2020.103971
- Rengaraj, S., Yeon, K. H., Kang, S. Y., Lee, J. U., Kim, K. W., and Moon, S. H. (2002). Studies on adsorptive removal of Co(II), Cr(III) and Ni(II) by IRN77 cation-exchange resin. *J. Hazard. Mater.* 92 (2), 185–198. doi:10.1016/s0304-3894(02)00018-3
- Shahryari, T., Mostafavi, A., Afzali, D., and Rahmati, M. (2019). Enhancing cadmium removal by low-cost nanocomposite adsorbents from aqueous solutions; a continuous system. *Compos. Part B-Engineering* 173, 106963. doi:10.1016/j.compositesb.2019.106963
- Song, C. Y., Jiao, Y. Y., Tian, Z. H., Qin, Q., Qin, S., Zhang, J., et al. (2022). Fabrication of hollow-fiber nanofiltration membrane with negative-positive dual-charged separation layer to remove low concentration CuSO₄. *Sep. Purif. Technol.* 296, 121352. doi:10.1016/j.seppur.2022.121352
- Vatanpour, V., Mansourpanah, Y., Khadem, S. S. M., Zinadini, S., Dizge, N., Ganjali, M. R., et al. (2021). Nanostructured polyethersulfone nanocomposite membranes for dual protein and dye separation: lower antifouling with lanthanum (III) vanadate nanosheets as a novel nanofiller. *Polym. Test.* 94, 107040. doi:10.1016/j.polymertesting.2020.107040
- Wang, M., Ye, H., Zheng, X., Chen, S., Xing, H., Tao, X., et al. (2023). Adsorption behaviors and mechanisms of simultaneous cadmium and fluoride removal on waste bovine bone from aqueous solution. *J. Environ. Chem. Eng.* 11 (1), 109035. doi:10.1016/j.jece.2022.109035
- Wen, Y., Xie, Z., Xue, S., Long, J., Shi, W., and Liu, Y. (2022). Preparation of novel polymethacryloyl hydrazone modified sodium alginate porous adsorbent with good stability and selective adsorption capacity towards metal ions. *Sep. Purif. Technol.* 303, 122184. doi:10.1016/j.seppur.2022.122184
- Wu, R. P. (2019). Removal of heavy metal ions from industrial wastewater based on chemical precipitation method. *Ekoloji* 28 (107), 2443–2452.
- Zhang, J., Xue, C. H., Ma, H. R., Ding, Y. R., and Jia, S. T. (2020). Fabrication of PAN electrospun nanofibers modified by tannin for effective removal of trace Cr(III) in organic complex from wastewater. *Polymers* 12 (1), 210. doi:10.3390/polym12010210
- Zhu, Y., Zheng, Y., Wang, F., and Wang, A. (2016). Fabrication of magnetic macroporous chitosan-g-poly (acrylic acid) hydrogel for removal of Cd²⁺ and Pb²⁺. *Int. J. Biol. Macromol.* 93, 483–492. doi:10.1016/j.ijbiomac.2016.09.005